Journal of Experimental Botany, Vol. 73, No. 18 pp. 6133–6149, 2022
https://doi.org/10.1093/jxb/erac247 Advance Access Publication 5 June 2022

RESEARCH PAPER

The transcription factor OsGATA6 regulates rice heading date and grain number per panicle

Yan-Jie Zhang[1,2], Yu Zhang[3], Liang-Li Zhang[3], Jun-Xian He[4], Hong-Wei Xue[2,5], Jia-Wei Wang[6] and Wen-Hui Lin[1,2,*]

[1] The Joint International Research Laboratory of Metabolic and Developmental Sciences, School of Life Sciences and Biotechnology, Shanghai Jiao Tong University, Shanghai, 200240, China
[2] Shanghai Collaborative Innovation Center of Agri-Seeds/Joint Center for Single Cell Biology, Shanghai Jiao Tong University, Shanghai, 200240, China
[3] State Key Laboratory of Plant Molecular Physiology, Institute of Botany, Chinese Academy of Sciences, Beijing, China
[4] School of Life Sciences and State Key Laboratory of Agrobiotechnology, The Chinese University of Hong Kong, Shatin, New Territories, Hong Kong, China
[5] School of Agriculture and Biology, Shanghai Jiao Tong University, Shanghai 200240, China
[6] National Key Laboratory of Plant Molecular Genetics, CAS Center for Excellence in Molecular Plant Sciences (CEMPS), Institute of Plant Physiology and Ecology, Chinese Academy of Sciences, Shanghai 200032, China

* Correspondence: whlin@sjtu.edu.cn

Received 29 November 2021; Editorial decision 26 May 2022; Accepted 2 June 2022

Editor: Rainer Melzer, University College Dublin, Ireland

Abstract

Heading date, panicle architecture, and grain size are key traits that affect the yield of rice (*Oryza sativa*). Here, we identified a new gene, *OsGATA6*, whose product regulates heading date. Overexpression of *OsGATA6* resulted in delayed heading, increased grain number, and decreased grain size. Knockdown lines generated by artificial microRNA (amiRNA) and CRISPR genome-edited lines of *OsGATA6* both showed earlier heading, decreased grain number, and increased grain size. These results suggested that OsGATA6 negatively regulates heading date, positively regulates panicle development, and affects grain size. *OsGATA6* was found to be constitutively expressed in rice, and strongly expressed in young leaves and panicles. *In situ* hybridization analyses showed that *OsGATA6* was specifically localized in superficial cells of the panicle primordium. Overexpression lines show decreased expression of *RFT1* and *Hd3a*, which promote heading. *OsMFT1*, which delays heading date and increases grain number, was down-regulated in amiRNA lines. Further analyses showed that OsGATA6 could bind to the promoter of *OsMFT1* and induce its expression, thereby regulating heading date and panicle development. Overexpression of *OsGATA6* in Arabidopsis resulted in repressed expression of *AtFT* and late flowering, suggesting that its function is similar. Taken together, we have identified a new GATA regulator that influences rice heading date and grain number, which potentially increases rice yield.

Keywords: Florigen, GATA transcription factor, grain number per panicle, grain size, heading date, *Oryza sativa*, rice.

Introduction

Increasing the total yield of rice (*Oryza sativa*) is a fundamental goal of crop breeding and production. The grain yield of rice is determined by several factors, including the panicle number per unit area, the grain number per panicle, and the individual grain weight (Sakamoto and Matsuoka, 2008; Xing and Zhang, 2010). Panicle number is closely related to plant architecture and tiller number, grain number is determined by panicle architecture and fertility, and grain weight is determined by grain development and filling. Among these factors, the grain number is particularly important for crop yield: increasing the grain number significantly enhances yield (Sakamoto and Matsuoka, 2008). The maximum grain number is determined by the branch that develops from the inflorescence meristem. The grain weight is positively correlated with grain size, as determined by grain length, width, and thickness (Huang *et al.*, 2013; Zuo and Li, 2014). Heading date is another key agronomic trait that affects rice yield. If it is too early, the shortened vegetative growth period leads to insufficient nutrient accumulation. If it is too late, defective filling and grain-set, which are affected by lower temperatures at the later stages of reproductive growth, lead to decreased final yield.

Rice is a facultative short-day (SD) plant in which heading is promoted under short-day conditions and inhibited under long-day (LD) conditions (Brambilla and Fornara, 2013; Zhou *et al.*, 2021). Florigen is a mobile floral signal that induces flowering in different species (Zeevaart *et al.*, 2006; Tamaki *et al.*, 2007). Under suitable conditions, florigen is produced in the leaves and transported to the shoot apical meristem, triggering heading (Tamaki *et al.*, 2007; Komiya *et al.*, 2009). There are two florigens in rice, encoded by *RICE FLOWERING LOCUS T 1* (*RFT1*) and *Heading date 3a* (*Hd3a*). Both belong to the phosphatidylethanolamine-binding protein (PEBP) gene family, and their overexpression has been shown to promote heading (Chardon and Damerval, 2005). At least two heading signaling pathways control florigen expression in rice, the *Heading date 1* (*Hd1*) pathway and the *Early heading date 1* (*Ehd1*) pathway. *Hd1* encodes a zinc finger protein (Brambilla and Fornara, 2013) whilst *Ehd1* encodes a B-type response regulator with a DNA-binding domain. Both Hd1 and Ehd1 induce *Hd3a* under SD conditions, and Ehd1 also induces *RFT1* under LD conditions (Zhou *et al.*, 2021). Most inhibitors of LD heading act via *Ehd1* (Brambilla and Fornara, 2013; Zhou *et al.*, 2021). *Ghd7* encodes a rice-specific CCT domain protein, and Ghd7 interacts with Hd1 to inhibit the expression of *Ehd1* and suppress heading under LD conditions (Nemoto *et al.*, 2016). *OsGIGANTEA* (*OsGI*) promotes the expression of *Hd1* under SD and LD conditions (Hayama *et al.*, 2002; Zhou *et al.*, 2021). In Arabidopsis, *FLOWERING LOCUS T* (*AtFT*) is the florigen and the homolog of *RFT1* and *Hd3a* (Chardon and Damerval, 2005). *CONSTANS* (*AtCO*) is homologous to *Hd1* (Brambilla and Fornara, 2013), and *GIGANTEA* (*AtGI*) encodes the ortholog of *OsGI* (Hayama *et al.*, 2002; Zhou *et al.*, 2021).

Several genes that regulate heading date also affect grain number and size, and hence have multiple functions in regulating rice yield. Compared with the wild type, the *ehd1 hd1* double-mutant has fewer primary branches and spikelets. In addition, both Ehd1 and Hd1 regulate panicle size by mediating the expression of *RFT1* and *Hd3a* in leaves at heading (Endo-Higashi and Izawa, 2011). This suggests that genes that regulate heading date also affect grain number per panicle and grain size. If this is the case, there should be correlations among the three yield-related traits (Wei *et al.*, 2010; Chen *et al.*, 2015).

Previous studies have identified several genes that affect rice panicle development and grain number. *ABERRANT PANICLE ORGANIZATION1* (*APO1*) encodes an F-box transcription factor, and its loss-of-function mutant produces fewer branches and spikelets (Ikeda *et al.*, 2005). *DENSE AND ERECT PANICLE 1* (*DEP1*) encodes a protein containing a PEBP domain. The mutant shows a shortened rachis length and produces increased numbers of primary and secondary branches and spikelets (Huang *et al.*, 2009). *DEP2* encodes a plant-specific protein that restricts cell proliferation and hinders rapid elongation of the rachis and branches (Li *et al.*, 2010). *LAX PANICLE1* (*LAX1*) encodes a bHLH transcription factor that affects the formation and maintenance of the panicle lateral primordium (Komatsu *et al.*, 2001). Among members of the *TERMINAL FLOWER 1/ CENTRORADIALIS* (*TFL1/CEN*) gene family, overexpression of *CEN1* and *CEN2* lead to an increased number of secondary branches and additional tertiary branches (Zhang *et al.*, 2005). *MOTHER OF FT AND TFL1* (*OsMFT1*) also encodes a PEBP family protein, and its loss-of-function mutant shows earlier heading and a reduced grain number (Song *et al.*, 2018). *FUWA* encodes a NHL domain-containing protein. The *fuwa* mutant has more compact and erect panicles and produces fewer grains, but the grains are shorter, wider, and thicker (Chen *et al.*, 2015).

GATA transcription factors are found in animals, fungi, and plants. GATA proteins recognize the conserved WGATAR motif (where W = T or A, and R = G or A) in target genes (Lowry and Atchley, 2000). GATA transcription factors are involved in the regulation of organ differentiation and development. Overexpression of *CYTOKININ-RESPONSE GATA TRANSCRIPTION FACTOR 1* (*CGA1*) in rice results in semi-dwarf plants with fewer tillers (Hudson *et al.*, 2013). Mutants of *NECK LEAF 1* (*NL1*) show delays in heading date, smaller panicles with overgrown bracts, and abnormal elongation patterns of upper internodes (Wang *et al.*, 2009). SHORT AND NARROW FLAG LEAF1 (SNFL1) regulates flag-leaf size in rice, and mutants show decreased length of epidermal cells and reduced number of longitudinal veins in the flag leaf (He *et al.*, 2018). Overexpression of *OsGATA12* causes increased leaf greenness and decreased

leaf and tiller numbers, and affects yield parameters (Lu *et al.*, 2017). Our previous research has found that *OsGATA7* is mediated by the phytohormone brassinosteroid (BR), which regulates rice plant architecture and grain shape (Zhang *et al.*, 2018).

Despite progress in understanding the regulatory mechanisms of heading date and panicle development, only a few genes with multiple functions regulating several agronomic traits have been identified. Here, we identified another GATA transcription factor, *OsGATA6*, which affects heading date, grain number, and grain size. We investigated its multiple functions and regulatory mechanisms in regulating heading date and grain number per panicle. Our findings suggest that this gene is a potential candidate for improving rice yield.

Materials and methods

Plant material and growth conditions

The wild type in this study was the *Oryza sativa* subsp. *japonica* rice variety Zhonghua 11 (ZH11). Phenotypic observations were conducted for plants grown in a paddy field in Shanghai, China, in June–October. Seedlings were also grown in a greenhouse under 14/10 h light/dark at 30/24 °C. Arabidopsis plants were grown in a greenhouse under 16/8 h light/ dark at 22°C.

Vector construction and genetic transformation

In all transformations with rice, the vectors were first transferred into *Agrobacterium* EHA105, and the positive clones were transformed into the corresponding plant material to obtain the transgenic lines (Zhang *et al.*, 2018).

To construct the overexpression (*OsGATA6*-OX) lines, the primer pair OsGATA6 OX-F/R was used to amplify the *OsGATA6* sequence from ZH11 genomic DNA using high-fidelity DNA polymerase (KFX-101, Toyobo). The product was digested with *Bam*HI/*Kpn*I, and then inserted into the pUN1301 vector (Li *et al.*, 2009). The final vector was transformed into ZH11 to obtain *OsGATA6*-OX lines. The primer pair OsGATA6 RT-F/ Noster-R was used for genotyping. All the primers used in this study are shown in Supplementary Table S1.

To obtain the artificial microRNA interference lines (amiRNA, *OsGATA6*-AM), three primer pairs Primer A/OsGATA6-II, OsGATA6-I/OsGATA6-IV, and OsGATA6-III/Primer B were designed using the WMD3-Web MicroRNA Designer (http://wmd3.weigelworld.org), and used to amplify PCR products from the template pNW55 plasmid (Warthmann *et al.*, 2008; Subaran *et al.*, 2016) using high-fidelity DNA polymerase (KFX-101, Toyobo). The three PCR products were then mixed and used as templates to perform overlapping PCR with the primer pair Primer A/Primer B. The gel-purified PCR products were then digested with *Kpn*I and *Bam*HI, and ligated into pUN1301 (Li *et al.*, 2009). The final vector was transformed into wild-type ZH11 to obtain the *OsGATA6*-AM lines. The primer pair Primer A/B was also used for genotyping.

To obtain the CRISPR-Cas9 genome-edited lines (*OsGATA6*-CRI), the primer pair OsGATA6-LP/RP was annealed and connected into vector pOs-sgRNA (Miao *et al.*, 2013). The fragments between two sites attL1 and attL2 of the intermediate vector pOs-sgRNA-OsGATA6, and two sites attR1 and attR2 of the vector pH-Ubi-cas9-7 (Miao *et al.*, 2013) were replaced to obtain the final vector pH-Ubi-cas9-7-OsGATA6 using Gateway recombination. The pH-Ubi-cas9-7-OsGATA6 plasmid was transformed into ZH11 to obtain the *OsGATA6*-CRI lines. The primer pair OsGATA6 CRI-F/R was used for genotyping. All procedures were carried out according to Miao *et al.* (2013).

The primer pair pGATA6-GUS F/R was used to amplify the 2368-bp sequence before the *OsGATA6* start codon from rice genomic DNA. The product was ligated into the intermediate vector pMD18-T (D101A, TaKaRa). Next, the pMD18-OsGATA6 and pCAMBIA1300+pBI101 vectors (Xing *et al.*, 2022) were double-digested with *Pst*I/*Bam*HI and ligated to obtain the final vector pCAMBIA+pBI101-OsGATA6, which was transformed into ZH11 to obtain the *pOsGATA6::GUS* line.

Using ZH11 genomic DNA as a template and OsGATA6 1302-F/-R as the primers, the KOD FX-amplified fragment was ligated into the pCAMBIA1302 vector (Liu *et al.*, 2003) after *Kpn*I/*Bgl*II double-digestion. After sequencing, the vector was transformed into ZH11 to obtain the *pOsGATA6::OsGATA6-GFP* line.

To observe the subcellular localization of OsGATA6, we constructed the vector pHB-OsGATA6-YFP. Using cDNA from the leaves of ZH11 as the template and pHB-OsGATA6-F/R as primers, a 1161-bp fragment was amplified using high-fidelity DNA polymerase KOD-Plus-Neo (KOD-401, Toyobo). The pHB-YFP vector was digested by *Spe*I, and the target fragment and the vector were connected using the In-Fusion method with a ClonExpress II One-Step Cloning Kit (C112-01, Vazyme). This yielded pHB-OsGATA6-YFP.

To obtain the *OsGATA6*-OX/*RFT1*-OX line, pUN1301-RFT1 was first constructed, then the *Ubiquitin* promoter and the CDS of *RFT1* were cut together and ligated into pCAMBIA2300 (Zhou *et al.*, 2020). The pCAMBIA2300-RFT1 vector was obtained. The *OsGATA6*-OX-11 line was transformed with pCAMBIA2300-RFT1 to obtain the double overexpression lines. The second selection marker was the kanamycin resistance gene Kan^R.

For the dual-luciferase assays, using ZH11 cDNA as the template and OsGATA6 Green-F/R as primers, the coding sequence of *OsGATA6* was amplified with KOD-Plus-Neo and ligated into the pGreen-35S plasmid (Li *et al.*, 2021) linearized with *Hin*dIII/*Eco*RI by the In-Fusion method. This yielded pGreen-35S-OsGATA6. Using ZH11 genomic DNA as the template and OsMFT1 LUC1/3/5-F/R as primers, three *OsMFT1* promoter fragments of different lengths were amplified with KOD-Plus-Neo. Each was ligated into the *Kpn*I/*Hin*dIII-linearized pGreenII 0800-Luc vector (Li *et al.*, 2021) using the In-Fusion method to obtain the three plasmids pGreenII 0800-LUC-OsMFT1-1/3/5. pGreenII 0800-LUC-RFT1-1/2/3 and pGreenII 0800-LUC-Hd3a-1/2 were constructed with RFT1 LUC1/2/3-F/R and Hd3a LUC1/2-F/R as primers in parallel. All the primers are shown in Supplementary Table S1, and the assays are described in detail below.

The *OsGATA6*-OX vector was transformed into the Arabidopsis wild-type Col-0 and into the BR-insensitive mutant *bri1-5* to obtain the Arabidopsis overexpression and complementary lines. Leaf morphology, main stem height, and other phenotypes of the complementary lines were recorded (Zhang *et al.*, 2018).

Quantitative real-time PCR analyses

Samples of young leaves, leaf sheaths,roots and stems from 4-week-old plants, and samples of older leaves, leaf sheaths, lamina joint and roots from 10-week-old plants, and young panicles (3–5 cm) of the wild-type ZH11 were quickly frozen in liquid nitrogen and ground to powder. RNA was extracted with TRIzol (15596-026, Invitrogen), quantified using a micronuclei acid analyser (Nanodrop 1000), and reverse-transcribed into cDNA using a FastKing RT Kit (with gDNase; KR116, Tiangen). Quantitative RT-PCR analyses were performed using a SYBR® Green Realtime PCR Master Mix Kit (QPK-201, Toyobo) and an Eppendorf Mastercycler® ep *realplex* quantitative PCR instrument.

The transcript levels of *OsGATA6* in the *OsGATA6*-OX and *OsGATA6*-AM lines were detected by qRT-PCR in the youngest leaves

on the main stem, which were collected from plants at 72 d after sowing in the paddy field (Shanghai) (Komiya *et al.*, 2009).

The transcript levels of *RFT1*, *Hd3a*, *Ghd7*, *Ehd1*, *Hd1*, *OsGI*, and *OsMFT1* in the youngest leaves were detected by qRT-PCR for 50-day-old plants of ZH11 and the *OsGATA6*-OX lines grown in the paddy field, for 60-day-old plants of ZH11 and the *OsGATA6*-AM and *OsGATA6*-CRI lines grown in the greenhouse, and for 35-day-old plants of all four lines grown in the greenhouse.

The transcript levels of *OsGATA6* in the Arabidopsis overexpression lines were detected by qRT-PCR in the inflorescences. The transcript levels of *AtFLC*, *AtFT*, *AtCO*, and *AtGI* were detected by qRT-PCR in rosette leaves of 4-week-old plants at the end of the light period.

The transcript levels of differentially expressed genes identified by microarray analysis (see below) were analysed by qRT-PCR using RNA from panicle primordia at the In2 stage (formation of primary branches I) and the In3 stage (formation of primary branches II).

The transcript levels of *OsGATA6* and the BR-responsive genes *OsD2* and *OsD11* were detected by qRT-PCR in 1-week-old ZH11 seedlings after 3 h of treatment (see below). The transcript levels of the BR-responsive genes *AtCPD* and *AtDWF4* were detected by qRT-PCR using RNA extracted from the inflorescences of the Arabidopsis complementary lines.

The transcript levels of *OsGATA6* in the Arabidopsis overexpression lines were calculated using the $2^{-\Delta CT}$ method, and those of other genes were calculated with the $2^{-\Delta\Delta CT}$ method. The primers used for the qRT-PCR analyses are shown in Supplementary Table S1.

Rice *OsACTIN1* (LOC_Os03g50885) and Arabidopsis *AtACTIN7* (AT5G09810) were used as the internal controls. The expression of *OsACTIN1* and *AtACTIN7* have both been shown to be stable under similar experimental conditions (Chu *et al.*, 2017; Gu *et al.*, 2017; Song *et al.*, 2019; Zheng *et al.*, 2019).

GUS staining analyses

Seedlings at 7-day-old, and young panicles at the P1–P4 stages (panicle development stages, delineated by panicle size; Jain *et al.*, 2007), spikelets from the panicles at the P1–P4 stages, and lamina joints of rice plants at 60-day-old were collected, immersed in GUS staining solution and placed in a vacuum pump for 20 min. The samples were then incubated overnight at 37 °C, after which they were decolorized in 75% ethanol at 37 °C. The GUS signals in the decolorized tissues were observed under a Leica DFC290 stereoscope and imaged using a Canon 600D camera.

Subcellular localization analyses

Positive *Agrobacterium* clones containing pHB-OsGATA6-YFP were cultured in kanamycin-containing YEB medium at 28 °C overnight. The cells were collected by centrifugation at room temperature and resuspended in injection buffer (half-strength MS medium, 10 mM MES, 10 mM $MgCl_2$, 200 μM acetosyringone) to OD_{600}=1. The solution was aspirated at room temperature in the dark for 2–3 h and then injected into leaves of tobacco (*Nicotiana benthamiana*). After growth in shade for 48 h, the leaves were cut from the plants, and the subcellular localization of OsGATA6 was observed under a Leica TCS SP8 laser confocal microscope.

The subcellular localization of OsGATA6 was also observed in the *pOsGATA6::OsGATA6-GFP* lines. The coleoptiles of 7-day-old seedlings were cut and observed under a Nikon A1 HD25 laser confocal microscope.

In situ hybridization

Specific regions of the *OsGATA6* sequence were selected to design the primer combinations GATA6 S-F/R and GATA6 A-F/R for sense and antisense probes, respectively. A DIG RNA labeling kit (Roche) was used for *in vitro* transcription of the probes. Panicle primordia of ZH11 were fixed with pre-cooled FAA (5% acetic acid, 50% ethanol, 3.7% formaldehyde) prepared using DEPC-treated ddH_2O, and then dehydrated using an ethanol gradient, embedded in paraffin, and sliced. Details of the hybridization process can be found in Li *et al.* (2006).

SEM analysis

Lemmas were collected and fixed with FAA (5% acetic acid, 50% ethanol, 3.7% formaldehyde) and SEM observations were performed as described previously (Zhang, *et al.* 2018). Cell lengths were measured using the ImageJ software.

Microarray analysis of differentially expressed genes related to yield traits

On the basis of the SEM observations, we selected panicle primordia at the In2–In3 stages (Ikeda *et al.*, 2004) from the wild-type ZH11 and the *OsGATA6*-AM lines and analysed differentially expressed genes using a rice expression profile chip (Agilent Technologies). Some of the genes identified were selected for verification of differential expression by qRT-PCR, as described above.

ChIP-PCR

ChIP-PCR analyses were conducted on young panicles (5–15 cm) of the *pOsGATA6::OsGATA6-GFP* lines and ZH11 using a GFP antibody (M20004, Abmart) and magnetic beads (16-663, Merck Millipore). The ChIP-PCR primers of *OsMFT1* are shown in Supplementary Table S1. Using the ChIP product as the template, quantitative ChIP-PCR was performed using a SYBR® Green Realtime PCR Master Mix Kit (QPK-201, Toyobo) and an Eppendorf Mastercycler® ep *realplex* quantitative PCR instrument as described by Jiang *et al.* (2013).

Dual-luciferase assays

pGreen-35S, pGreen-35S-OsGATA6, pGreenII 0800-LUC-OsMFT1-1/3/5, and pSoup-p19 (mass ratio 1:4) were co-transformed into *Agrobacterium* GV3101, and the positive clones were cultured in kanamycin/tetracycline/rifampycin resistance YEB medium at 28 °C overnight until OD_{600}=1–2. The cells were collected by centrifugation at room temperature and resuspended in injection buffer (half-strength MS medium, 10 mM MES, 10 mM $MgCl_2$, 200 μM acetosyringone) to OD_{600}=1. Then, pGreen-35S/35S-OsGATA6+pSoup-p19 and pGreenII 0800-LUC-OsMFT1-1/3/5+pSoup-p19 were mixed at a volume ratio of 4:1, and the mixture was left at room temperature in the dark for 2–3 h. The solution was aspirated and injected into tobacco leaves. After 48–72 h in the shade, the injection areas were cut, quickly frozen in liquid nitrogen, and ground. The samples were using a Dual-Luciferase® Reporter Assay System (E1910, Promega) according to the manufacturer's instructions, and sample readings were obtained using a GloMax® 20/20 Luminometer (E5311, Promega).

Dual-luciferase assays for *RFT1* and *Hd3a* were conducted in the same way as for *OsMFT1* but pGreenII 0800-LUC-OsMFT1-1/3/5 was replaced with pGreenII 0800-LUC-RFT1-1/2/3 and pGreenII 0800-LUC-Hd3a-1/2, respectively.

BR treatment

Seedlings of ZH11 at 1-week-old were immersed in 1 μM eBL and ddH_2O for 3 h, after which the transcript levels of *OsGATA6*, *OsD2*, and

OsD11 were detected by qRT-PCR using the primers listed in Supplementary Table S1.

To examine BR sensitivity, seeds of ZH11 and the *OsGATA6*-OX and *OsGATA6*-CRI lines were germinated in distilled water for 2 d. Seeds with consistent germination status were placed in 96-well plates, grown in 1 mM $CaCl_2$ solution for 4 d, and then transferred into 1 mM $CaCl_2$ solution with different concentrations of eBL for 6 d. The seedlings were cultured in the greenhouse. The root lengths of each line at the different eBL concentrations were measured, with 12 replicate seedlings being used, as described by Zhang *et al.* (2018).

Accession numbers

Genes referenced in this article can be found in Rice Genome Annotation Project (TIGR) and The Arabidopsis Information Resource (TAIR) under the following accession numbers: *OsGATA6* (LOC_Os01g54210), *OsMFT1* (LOC_Os06g30370), *RFT1* (LOC_Os06g06300), *Hd3a* (LOC_Os06g06320), *Ehd1* (LOC_Os10g32600), *Hd1* (LOC_Os06g16370), *OsGI* (LOC_Os01g08700), *Ghd7* (LOC_Os07g15770), *OsD2* (LOC_Os01g10040), *OsD11* (LOC_Os04g39430), *OsRCN2* (LOC_Os02g32950), *OsRCN4* (LOC_Os04g33570), *OsFTL1* (LOC_Os01g11940), *OsFTL13* (LOC_Os02g13830), *AtFLC* (AT5G10140), *AtFT* (AT1G65480), *AtCO* (AT5G15840), *AtGI* (AT1G22770), *AtCPD* (AT5G05690) and *AtDWF4* (AT3G50660).

Results

Cloning of OsGATA6

Our previous work showed that GATA transcription factors integrate the light- and brassinosteroid-signaling pathways, modulate brassinosteroid-mediated growth regulation, and influence architecture and grain shape (Luo *et al.* 2010; Zhang *et al.* 2018). Our cooperation work also identified a new GATA transcription factor, *OsGATA6* (LOC_Os01g54210), that is involved in the development of ground and vascular tissue in rice root tips (Zhang *et al*, 2021). In this current study, we further explored the function of *OsGATA6* in reproductive growth. Sequence analyses revealed that *OsGATA6* contains two exons of 291 bp and 873 bp and an intron of 510 bp (Supplementary Fig. S1A), and encodes a protein consisting of 387 amino acids. In addition, analyses using tools at the SMART website (http://smart.embl-heidelberg.de/) showed that OsGATA6 contains a conserved ZnFGATA region and seven low-complexity regions (Supplementary Fig. S1B).

Expression patterns of OsGATA6

Analyses at the Rice eFP Browser (http://bar.utoronto.ca/efprice/cgi-bin/efpWeb.cgi) indicated that transcription of *OsGATA6* is high in young panicles at the P1 stage, increases at the P2, P3, and P4 stages, then decreases at the later P5 and P6 stages, where P1 is early panicle development and P2–P6 are panicle development stages delineated by panicle size (Supplementary Fig. S2A) (Jain *et al.*, 2007). We conducted qRT-PCR analyses to quantify *OsGATA6* transcript levels in various tissues of the wild-type cultivar ZH11. Transcripts were detected in all of the tissues, with the highest levels in young leaf sheaths, young stems, old and young roots, and in the panicles (Supplementary Fig. S2B). GUS staining assays showed that *OsGATA6* was barely detectable in young panicles at the P1 and early P2 stages (the 1st and 2nd young panicles), was weak in the tips of young panicles at the P2–P3 stages (the 3rd and 4th panicles), but was intense in young panicles at the P4 stage (the 5th and 6th panicles) (Supplementary Fig. S2C). The GUS signal gradually became stronger in the glumes as the spikelets grew larger (Supplementary Fig. S2C). GUS signals were also detected in the leaf tip and roots of 7-day-old seedlings and in the lamina joints of 60-day-old plants (Supplementary Fig. S2C). These results indicated that *OsGATA6* might function in the panicle, spikelets, and in seedlings. *In situ* hybridization analyses showed that the expression of *OsGATA6* was limited to the margins of the panicle axis meristem at the In2 stage, to the margins of the primary branch primordium at the In3 stage, and to the margins of the differentiating branches at the In5 stage (formation of higher-order branches, Supplementary Fig. S2D–F) (Ikeda *et al.*, 2004). These results indicated that *OsGATA6* was expressed during the initial and subsequent developmental stages of the panicle primordia, especially at the margins. The tissue-specificity of *OsGATA6* in the panicle primordium was different to that previously found in the root apical meristem (Zhang *et al.*, 2021). We also examined the subcellular localization of OsGATA6 and, as expected, found that it was specifically localized in the nucleus (Supplementary Fig. S2H, I), consistent with its putative role as a transcription factor.

OsGATA6 negatively regulates heading date in rice

For the functional characterization of *OsGATA6*, we constructed overexpression (*OsGATA6*-OX), artificial microRNA interference (amiRNA, *OsGATA6*-AM), and CRISPR-Cas9 genome-edited (*OsGATA6*-CRI) lines, obtaining 21, 14, and 8 positive lines, respectively. We selected three lines of each type for further analysis (Supplementary Fig. S3). The *OsGATA6*-OX lines clearly showed delayed heading, while *OsGATA6*-AM and *OsGATA6*-CRI showed early heading (Fig. 1A, B), and the transcript levels of *OsGATA6* were significantly increased in the OX lines and reduced in the AM lines ($P<0.05$) (Fig. 1C, D). In the CRI lines, line 1 was homozygous with a 2-bp AG deletion at positions 17–18, line 2 was homozygous with a 60-bp deletion from position −7 to +53, and line 5 was also homozygous with a single base A insertion at position 18 (Fig. 1E). We constructed a vector containing the entire genomic sequence of *OsGATA6* driven by its native promoter and fused it with a GFP tag. The transgenic lines harboring *pOsGATA6::GATA6-GFP* also showed a late-heading phenotype (Supplementary Fig. S4A).

Overall, these results showed that *OsGATA6* was a negative regulator of rice heading date, that its overexpression led to significantly late heading, and that knockdown or genome-editing of *OsGATA6* led to early heading.

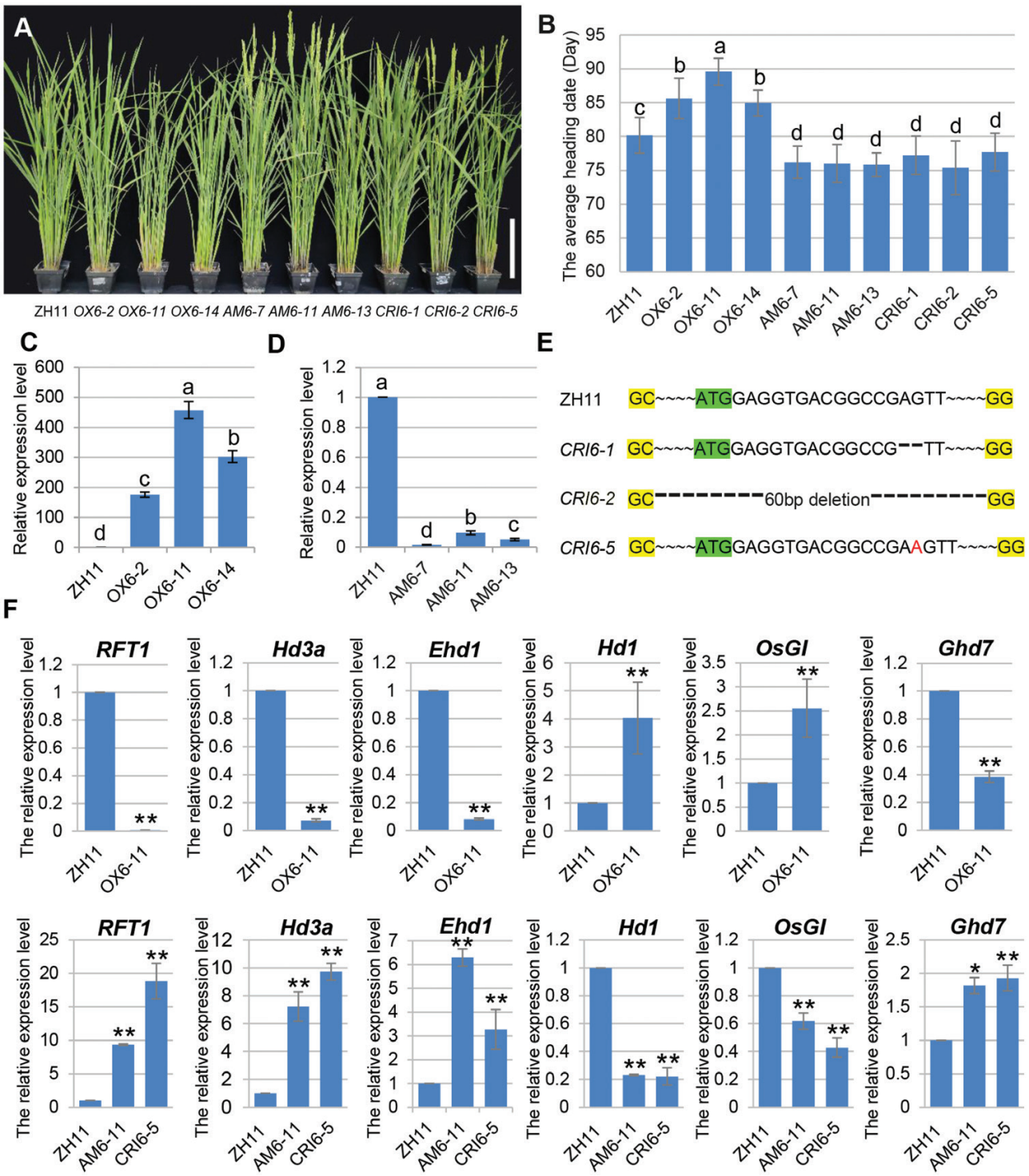

Fig. 1. Heading date of the rice wild-type ZH11 and overexpression, knockdown, and CRISPR-Cas9 lines of *OsGATA6*. (A) Representative images of plants at 80-day-old, showing the late heading date of the overexpression (OX) lines, and the early heading dates of the artificial microRNA interference (AM) knockdown and CRISPR-Cas9 (CRI) lines. The scale bar is 20 cm. (B) Mean heading dates in ZH11 and the overexpression, knockdown, and CRISPR-Cas9 lines. Data are means (±SE), *n*=17–38. (C) Relative expression levels of *OsGATA6* in the leaves of plants at 72 d after sowing of ZH11 and (C) the overexpression lines and (D) the knockdown lines. Data are means (±SE), *n*=3. (E) Sequencing results for the *OsGATA6* CRISPR-Cas9 lines. (F) Relative expression levels of *RFT1*, *Hd3a*, *Ehd1*, *Hd1*, *OsGI*, and *Ghd7* in leaves of ZH11 and the overexpression, knockdown and CRISPR-Cas9 lines. Data are means (±SE), *n*=3. Expression in the OX lines was determined in leaves of 50-day-old plants grown in the paddy field, whilst expression in the AM and CRI plants was determined in leaves of 60-day-old plants grown in the greenhouse. In (B–D) different letters indicate significant differences among means as determined using one-way ANOVA followed by Tukey's post-hoc test ($P<0.05$). In (F) significant differences compared with ZH11 were determined using Student's *t*-test: $^{*}P<0.05$, $^{**}P<0.01$.

OsGATA6 affects the expression of genes related to heading date in rice

To further examine the functioning of OsGATA6, we determined the transcript levels of genes involved in the regulation of heading date in the leaves of the wild-type ZH11 and the *OsGATA6*-OX, *OsGATA6*-AM, and *OsGATA6*-CRI lines. One of each of the three lines was selected for this analysis, and expression was determined in 50-day-old plants of ZH11 and the *OsGATA6*-OX lines grown in the paddy field, and for 60-day-old plants of ZH11 and the *OsGATA6*-AM and *OsGATA6*-CRI lines grown in the greenhouse. Compared with ZH11, *OsGATA6*-OX showed significantly lower transcript levels of *RFT1*, *Hd3a*, and *Ehd1* (Fig. 1F), while *OsGATA6*-AM and *OsGATA6*-CRI showed significantly higher levels ($P<0.01$). The transcript levels of *Hd1* and *OsGI* were both increased in *OsGATA6*-OX whereas they were decreased in *OsGATA6*-AM and *OsGATA6*-CRI. The transcript level of *Gh7d* (Xue *et al.*, 2008) was decreased in *OsGATA6*-OX and increased in *OsGATA6*-AM and *OsGATA6*-CRI compared with ZH11. We also detected the transcript levels of the six genes in leaves of 35-day-old plants of the same lines, but found that differences between ZH11 and transgenic lines were much less apparent (Supplementary Fig. S5). Previous studies have shown that florigen is transported from the leaves to the shoot apical meristem before heading (Tamaki *et al.*, 2007; Komiya *et al.*, 2009), and hence we deduce that in 35-day-old plants is too early to detect the different transcription levels of genes regulating heading date. Overall, our results suggest that OsGATA6 regulates rice heading date by modulating the transcription levels of genes in the leaves before heading, especially the core florigens *RFT1* and *Hd3a*.

OsGATA6 negatively regulates flowering time in Arabidopsis

We transformed the *OsGATA6*-OX vector into Arabidopsis Col-0 to determine whether its function was similar in regulating flowering time. A total of 11 T_1 transgenic lines were identified, and three lines with significantly increased transcript levels of *OsGATA6* were selected for phenotype analysis (Fig. 2A). Under LD conditions, all the wild-type plants flowered before 38 d after germination (DAG), but none of the three transgenic lines flowered. At 40 DAG, one of the transgenic lines was flowering but the other two were not (Fig. 2A). The *OsGATA6*-OX Arabidopsis plants showed significantly higher transcript levels and delayed flowering compared with the wild-type Col-0 ($P<0.05$) (Fig. 2B, C). The mean number of rosette leaves at flowering time (Amasino, 2010) was 15.41 in the wild type, and 17.47, 21.82, and 19.83 in the *OsGATA6*-OX lines 6, 8, and 10, respectively. We also calculated the percentage of flowering plants on different days of the wild type and the three transgenic lines in another batch. The wild type started flowering at 35 DAG, and all plants were flowering at 43 DAG (Fig. 2D). In contrast, transgenic line 6 started flowering at 41 DAG, and all plants were flowering at 47 DAG. Lines 8 and 10 both started flowering at 43 DAG, and all the plants in these lines were flowering at 51 DAG. Thus, compared with wild type, the three *OsGATA6*-OX lines showed significantly delayed flowering. These results indicated that *OsGATA6* could also negatively regulate flowering time in Arabidopsis.

To investigate the regulatory mechanism by which OsGATA6 controlled flowering in Arabidopsis, we determined the transcript levels of genes involved in the flowering pathway. Compared with Col-0, *AtFLC* was significantly up-regulated (Fig. 2E) and *AtFT* was down-regulated ($P<0.05$) (Fig. 2F), whilst *AtCO* and *AtGI* were slightly up-regulated (Fig. 2G, H) (Takashi and Yoshibumi,1993). In Arabidopsis, flowering is negatively regulated by *AtFLC* and positively regulated by *AtFT* (Fornara *et al.*, 2010). We therefore deduced that overexpression of *OsGATA6* in Arabidopsis delayed flowering by up-regulating *AtFLC* and down-regulating *AtFT*. *AtFT* is a close homolog of *RFT1* and *Hd3a*, suggesting that the regulatory mechanism of OsGATA6 is similar in rice and Arabidopsis.

Because overexpression of *OsGATA6* repressed expression of *RFT1*, we overexpressed *RFT1* in rice *OsGATA6*-OX lines. These double overexpression lines headed earlier than the *OsGATA6*-OX lines, and some individual plants even headed on rooting medium during transformation (Supplementary Fig. S4B). This indicated that *RFT1* might act downstream of *OsGATA6*.

OsGATA6 regulates grain number per panicle

Phenotypic analyses indicated that *OsGATA6* also affected the grain number per panicle. Compared with ZH11, the three *OsGATA6*-OX lines showed a more compact panicle architecture (Fig. 3A), significantly increased numbers of primary and secondary branches ($P<0.05$) (Fig. 3E, F), and higher grain numbers per panicle ($P<0.05$) (Fig. 3B, G). As a result, the total grain number per panicle was significantly higher in the *OsGATA6*-OX lines than in ZH11. In contrast, compared with ZH11, the three *OsGATA6*-AM lines showed a much sparser panicle architecture (Fig. 3C) with significantly fewer secondary branches (Fig. 3E, F), and fewer grains per panicle (Fig. 3D, G). Hence, the total number of grains per panicle was decreased in the *OsGATA6*-AM lines.

The panicle architecture was similar between the *OsGATA6*-CRI and *OsGATA6*-AM lines. Compared with ZH11, the three *OsGATA6*-CRI lines had a much sparser panicle architecture, fewer grains per panicle (Fig. 3H, I), and significantly fewer primary and secondary branches ($P<0.05$) (Fig. 3J, K). In addition, the total grain number per panicle was considerably lower in the three *OsGATA6*-CRI lines ($P<0.05$) (Fig. 3L). Overall, our results demonstrated that OsGATA6 positively regulated panicle development and grain number.

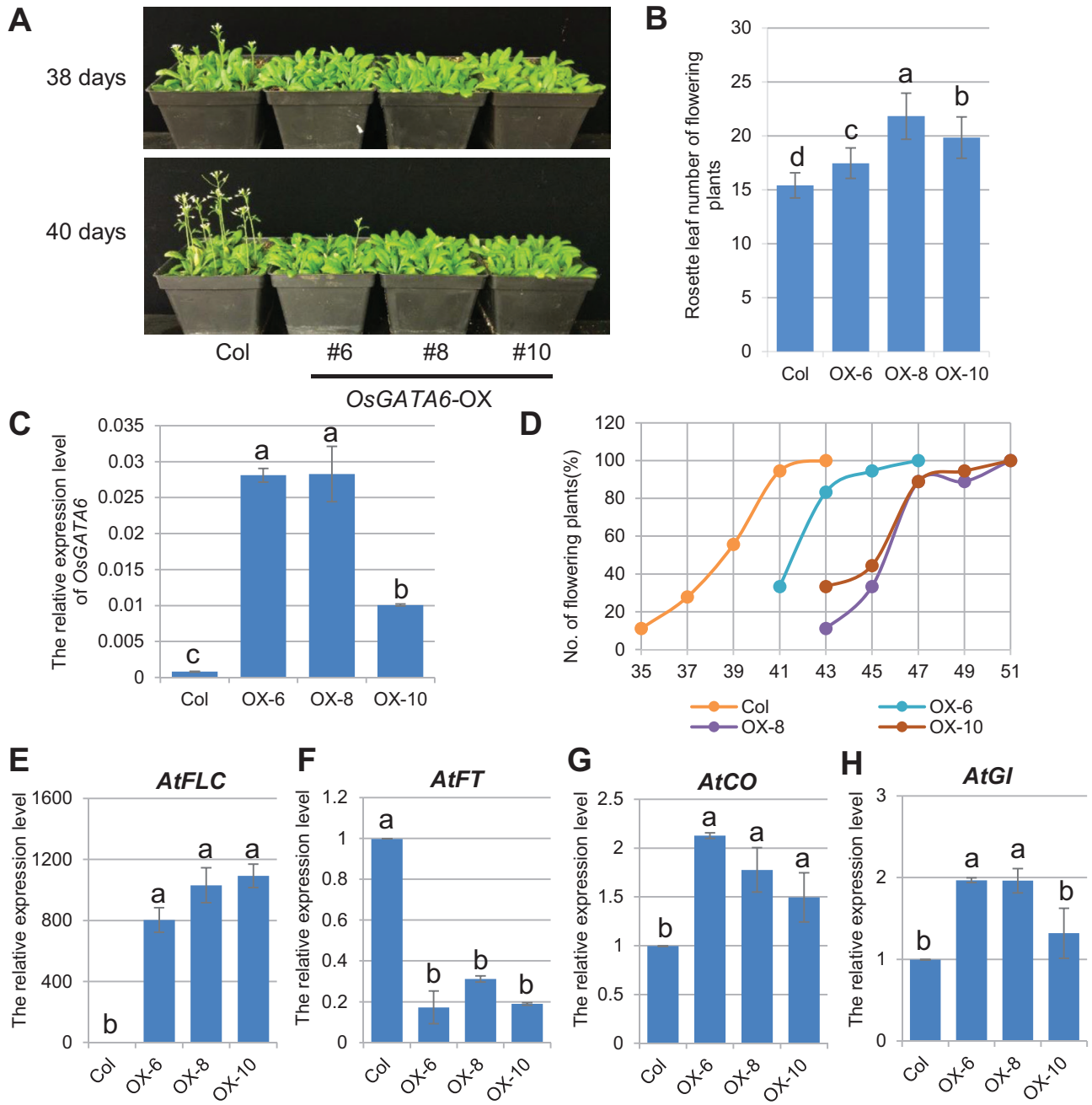

Fig. 2. Flowering of the Arabidopsis Col-0 wild-type and transgenic plants overexpressing *OsGATA6*. (A) Representative images of Col and three *OsGATA6* overexpression (OX) lines at 38- and 40-day-old. (B) Flowering time expressed as mean rosette leaf number in Col and the *OsGATA6*-OX lines. Data are means (±SE), *n*=17–18. (C) The relative expression levels of *OsGATA6* in Col and the *OsGATA6*-OX lines in the inflorescences. (D) Progression of flowering with time in Col and the *OsGATA6*-OX lines. The percentage of plants flowering was assessed every 2 d for a population of 18 plants per genotype. (E–H) Relative expression levels of genes involved in the flowering pathway in the rosette leaves of 4-week-old plants of Col and the *OsGATA6*-OX lines. (E) *AtFLC*, (F) *AtFT*, (G) *AtCO*, and (H) *AtGI*. Data in (C) and (E–H) are means (±SE), *n*=3. Different letters indicate significant differences among means as determined using one-way ANOVA followed by Tukey's post-hoc test ($P<0.05$).

OsGATA6 regulates grain size

Examination of individual grains revealed that OsGATA6 regulated not only grain number per panicle but also grain size, with those of the *OsGATA6*-OX lines being smaller. The mean grain lengths and widths of the *OsGATA6*-OX grains were shorter than those of ZH11 ($P<0.05$) (Fig. 4A–D). Conversely, the grains of the *OsGATA6*-AM lines were larger than those of ZH11, with the mean lengths and widths being longer than those of ZH11. We also obtained similar results for brown

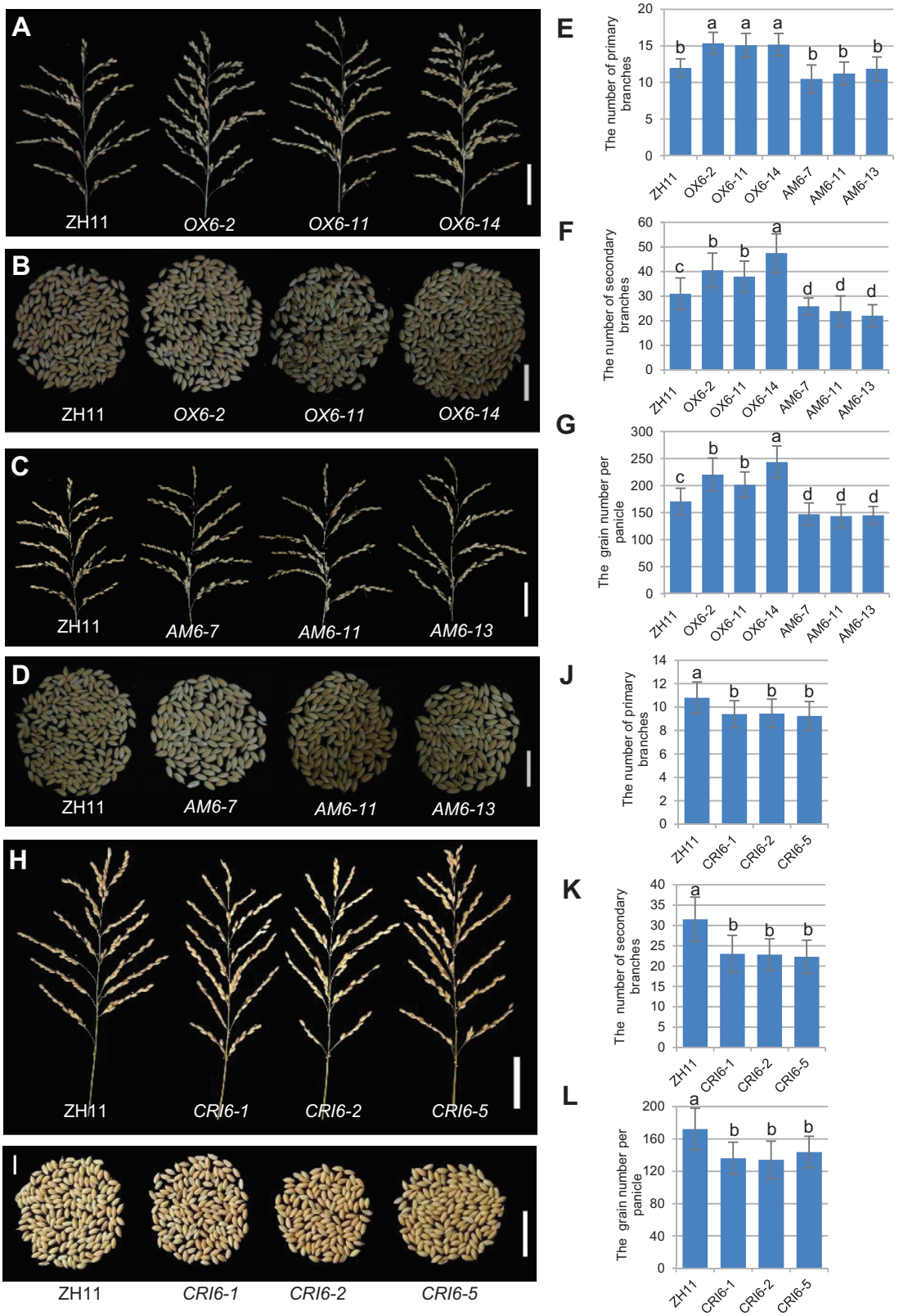

Fig. 3. Panicle architecture and grain numbers of the rice wild-type ZH11 and overexpression, knockdown, and CRISPR-Cas9 lines of *OsGATA6*. (A) Panicles and (B) the corresponding grains of ZH11 and three *OsGATA6* overexpression (OX) lines. (C) Panicles and (D) the corresponding grains of ZH11 and three artificial microRNA interference (AM) *OsGATA6*-knockdown lines. The scale bars are 4 cm in (A, C) and 2 cm in (B, D). (E) The numbers of primary branches and (F) secondary branches in ZH11 and the overexpression and knockdown lines. (G) The grain numbers per panicle in ZH11 and

the overexpression and knockdown lines. Data are means (±SE), n=21–25. (H) Panicles and (I) the corresponding grains of ZH11 and three *OsGATA6* CRISPR-Cas9 (CRI) lines. The scale bars are 5 cm in (H) and 3 cm in (I). (J) The numbers of primary and (K) secondary branches in ZH11 and the CRISPR-Cas9 lines. (L) The grain numbers per panicle in ZH11 and the CRISPR-Cas9 lines. Data are means (±SE), n=32–41 in (J), n=27–30 in (K), and n=31–35 in (L). Different letters indicate significant differences among means as determined using one-way ANOVA followed by Tukey's post-hoc test (P<0.05).

rice. The mean lengths and widths of *OsGATA6*-OX brown rice were shorter than those of ZH11 (P<0.05) (Supplementary Fig. S6A, D, G) whilst the length of *OsGATA6*-AM brown rice was longer (P<0.05) (Supplementary Fig. S6B, E). The *OsGATA6*-CRI lines showed a similar increase in grain size as the *OsGATA6*-AM lines, regardless of whether the glumes were included or not (P<0.05) (Fig. 4F–I; Supplementary Fig. S6C, F). Examination using SEM showed no significant differences in cell length among the wild type and the other three lines (Supplementary Fig. S7), which indicated that *OsGATA6* influenced grain size mainly through cell proliferation, not cell expansion.

Compared with ZH11, the *OsGATA6*-OX lines showed a lower 1000-grain weight, and the *OsGATA6*-AM and the *OsGATA6*-CRI lines showed a higher 1000-grain weight (Fig. 4E, J), indicating that the expression level of *OsGATA6* was negatively correlated with grain weight.

Transcriptome analysis of differentially expressed genes in panicle primordia of OsGATA6-*AM lines*

Previous studies have shown that some genes expressed in early primordia regulate heading date, grain number per panicle, and grain size (Endo-Higashi and Izawa, 2011). To explore the regulatory mechanism underlying the multiple functions of OsGATA6, we first compared the panicle primordia of ZH11, *OsGATA6*-OX lines, and *OsGATA6*-AM lines by SEM, and found phenotypic differences among the lines at the In3 stage. The *OsGATA6*-OX lines had more primary primordia that were more densely arranged compared with ZH11, while the *OsGATA6*-AM lines had the opposite phenotype of fewer, more sparsely arranged primary primordia (Fig. 5A).

To investigate how OsGATA6 regulates heading date, grain number per panicle, and grain phenotype, we collected primordia of ZH11 and the *OsGATA6*-AM lines at the In2 and In3 stages and analysed gene expression using a rice expression profiling chip. We used the *OsGATA6*-AM lines for transcriptome analysis because we obtained them earlier than the other lines. Compared with ZH11, the *OsGATA6*-AM lines had 818 up-regulated genes and 284 down-regulated genes (Fig. 5B). A volcano plot was generated to illustrate the magnitude of differences in gene expression levels, the distribution of P-values, and the distribution of the differentially expressed genes (DEGs) (Fig. 5C; Supplementary Table S2). A bubble chart of GO enrichment was generated to display the most significant 30 terms among the three categories of 'biological process', 'cell composition', and 'molecular function', which indicated that DNA-binding transcription factor activity was the most significant, and many processes related to transcriptional regulation and RNA modification were also enriched in the DEGs (Fig. 5D). Given that *OsGATA6* encodes a putative transcription factor that regulates grain number per panicle and grain size, which are related to cell growth, the results of the GO enrichment analysis provided reasonable explanations of its functions. Most of the significant items identified in our KEGG analysis were biosynthesis and metabolism genes (Fig. 5E), indicating that OsGATA6 regulates panicle and spikelet development, possibly through active biosynthesis and metabolism of essential molecules. For example, the first group of identified genes was connected to phenylpropanoid biosynthesis, and phenylpropanoids are a group of plant secondary metabolites derived from phenylalanine that have various structural and signaling functions. The product of the phenylalanine pathway is the starting compound for the synthesis of lignin, which is particularly important in the formation of cell walls. In addition, cell proliferation and expansion are essential for spikelet growth (Li and Li, 2016). These results further suggested that OsGATA6 functions as a transcription factor to promote cell growth.

Based on the above analysis, we further analysed the expression patterns of selected DEGs, namely the PEBP family genes *OsMFT1*, *OsRCN2*, *OsRCN4*, *OsFTL1*, and *OsFTL13*. We found that *OsMFT1*, *OsRCN2*, and *OsFTL13* were down-regulated, whilst *OsRCN4* and *OsFTL1* were up-regulated in *OsGATA6*-AM (Fig. 5F), suggesting that genes in the PEBP family probably act downstream of *OsGATA6*. Previous studies have shown that *OsMFT1* regulates not only heading date but also spikelets per panicle: CRISPR-Cas9 lines of *OsMFT1* show early heading, more sparsely arranged panicles, and decreased grain number, while overexpression lines show the opposite phenotypes (Song *et al.*, 2018). These phenotypes of *OsMFT1*-disrupted lines were similar to those that we found in the *OsGATA6*-disrupted lines. We also found that the transcript levels of *OsMFT1* in the leaves were decreased in the *OsGATA6*-AM and *OsGATA6*-CRI lines compared with the wild type (Supplementary Fig. S5G, H). Therefore, we speculated that OsMFT1 might mediate the functions of OsGATA6 in regulating heading date and grain number per panicle, and subsequently grain size.

OsGATA6 specifically regulates OsMFT1

We searched for putative GATA transcription factor binding sites in the *OsMFT1* genome sequence and detected 10 potential target sites in the 2.5-kb promoter region upstream of the start codon, and one and three sites in the intron and the

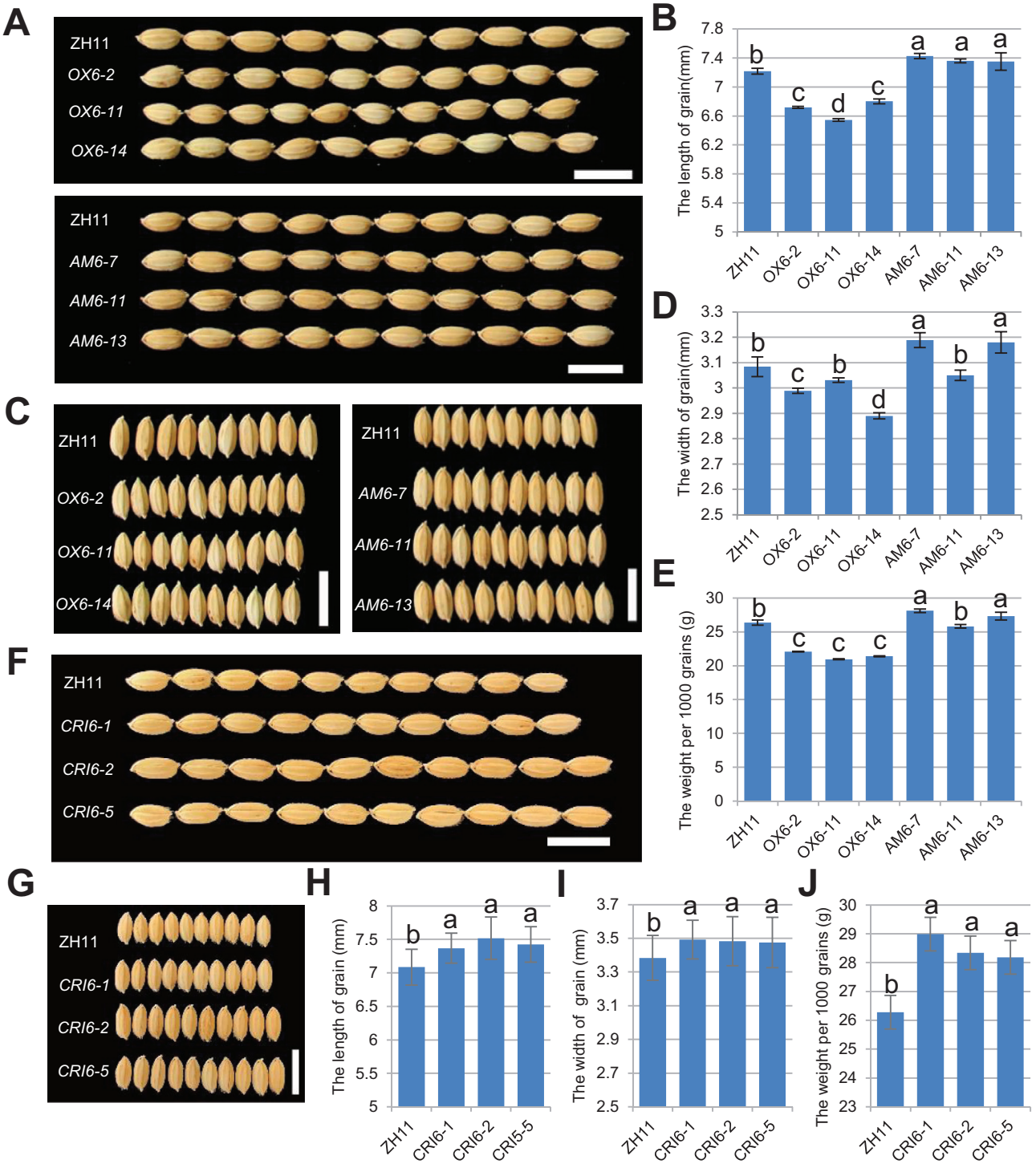

Fig. 4. Grain size in the rice wild-type ZH11 and overexpression, knockdown, and CRISPR-Cas9 lines of *OsGATA6*. (A) Grain length in ZH11 and the *OsGATA6* overexpression (OX) and artificial microRNA interference (AM) knockdown lines. (B) Mean grain length in ZH11 and the overexpression and knockdown lines. (C) Grain width in the overexpression and knockdown lines. (D) Mean grain width in ZH11 and the overexpression and knockdown lines, and (E) 1000-grain weight. (F) Grain length in ZH11 and the CRISPR-Cas9 lines CRI, and (G) grain width. (H) Mean grain length in ZH11 and the CRISPR-Cas9 lines, (I) mean grain width, and (J) 1000-grain weight in CRISPR-cas9 lines. All scale bars are 1 cm. Data are means (±SE), n=280–722) in (B, D, E), and n=33–83 in (H–J). Different letters indicate significant differences among means as determined using one-way ANOVA followed by Tukey's post-hoc test (P<0.05).

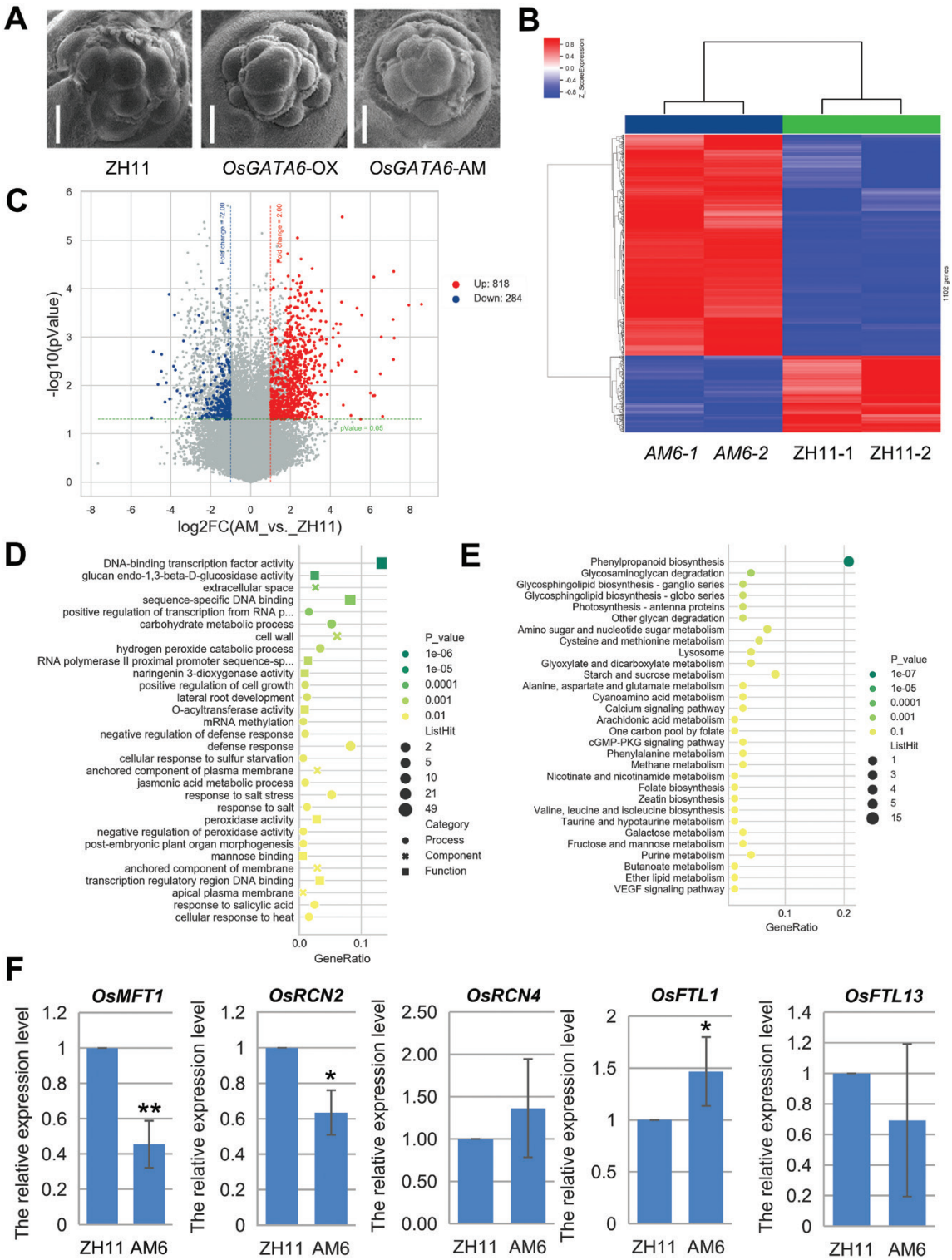

Fig. 5. Microarray analysis of differentially expressed genes between the rice wild-type ZH11 and *OsGATA6* knockdown lines. (A) SEM images of primary branch primordia at the In3 stage in ZH11 and an *OsGATA6* overexpression (OX) line and an artificial microRNA interference (AM) knockdown line. (B) Hierarchical clustering of differentially expressed genes (DEGs) between ZH11 and *OsGATA6*-AM. (C) Volcano plot showing the final screening and distribution of DEGs. (D) Bubble chart of the top 30 terms with the smallest *P*-values in GO enrichment analysis. (E) Bubble chart displaying KEGG enrichment analysis of the DEGs. (F) Transcript levels of *OsMFT1*, *OsRCN2*, *OsRCN4*, *OsTFL1*, and *OsTFL13* in ZH11 and *OsGATA6*-AM primordia. Data are means (±SE) from three biological replicates. Significant differences were determined using Student's *t*-test: **P*<0.05, ***P*<0.01.

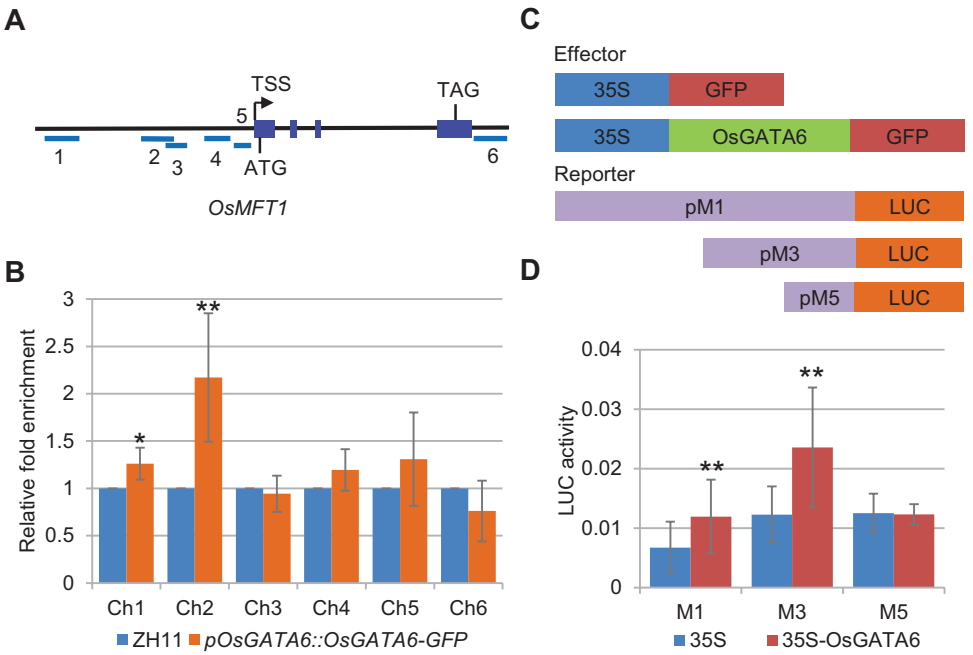

Fig. 6. Chromatin immunoprecipitation and dual-luciferase assays. (A) Diagram of the *OsMFT1* genomic sequence showing the fragments used. (B) ChIP quantitative PCR analysis using young panicles of the rice wild-type ZH11 and the *pOsGATA6::OsGATA6-GFP* line showing OsGATA6 binding to the fragments of the *OsMFT1* promoter. Data are from three biological replicates. (C) Diagrams of the effector and reporter constructs used for dual-luciferase assays. The regions pM1, pM3, and pM5 correspond to fragments 1, 3, and 5 in (A) and are the promoter sequences from the 5′end of the fragments. (D) Luciferase activities with different combinations of reporters and effectors. Data are from 10 biological replicates. Significant differences between means were determined using Student's *t*-test: **P*<0.05, ***P*<0.01.

3′-UTR, respectively. We then conducted ChIP analyses using the young panicles of the *pOsGATA6::OsGATA6-GFP* lines with the aim of determining whether OsGATA6 could target the *OsMFT1* sequence *in vivo*. The ChIP analyses indeed showed that the OsGATA6 protein could target the *OsMFT1* promoter directly, and the target sites were located in the first and second fragments, and possibly in the fifth fragment (Fig. 6A, B). Based on these results, the *OsMFT1* promoter sequence was divided into three fragments with different lengths, pM1/3/5 (Fig. 6C), corresponding to the respective fragments used in the ChIP analysis. Dual-luciferase assays were then conducted to test the transcriptional regulation activity of OsGATA6 in tobacco leaves. The results showed that OsGATA6 induced *LUC* expression when it was driven by the full-length sequence (M1) and the short-deleted sequence (M3) of the *OsMFT1* promoter, but not when it was driven by the long-deleted sequence (M5) (Fig. 6D). There were seven possible GATA transcription factor binding sites between the M3 and M5 fragments of the *OsMFT1* promoter, and four of them in the second fragment were also identified by the ChIP assays. We concluded that these four functional *cis*-elements were responsible for the transcriptional activation of *OsMFT1* by OsGATA6. Since OsMFT1 delays heading date and positively regulates grain number (Song *et al.*, 2018), we concluded that OsGATA6 regulates the heading date and grain number per panicle mainly by up-regulating the transcription of *OsMFT1* (Fig. 7).

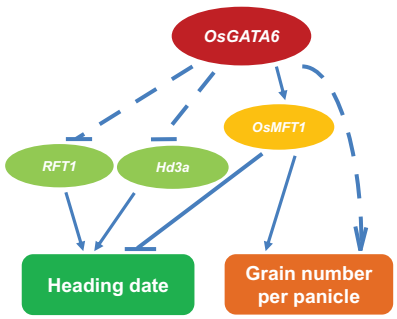

Fig. 7. Proposed model of how OsGATA6 regulates heading date and grain number per panicle in rice. *RFT1* and *Hd3a* act to promote heading, and expression of *OsGATA6* results in their decreased transcription, thereby delaying heading. Meanwhile, OsGATA6 directly targets the promoter region of *OsMFT1* and induces its transcription, which results in a delay in heading date and an increase in grain number per panicle. It is also possible that OsGATA6 regulates grain number via other mechanisms.

OsGATA6 regulates plant growth and development in a BR-related manner

GATA regulators have previously been reported to be involved in brassinosteroid (BR) signaling (Luo *et al.*, 2010; Zhang *et al.*, 2018), and therefore, we investigated whether OsGATA6 is also involved in BR signaling.

One-week-old seedlings of ZH11 were treated with 1 μM eBL solution for 3 h, and subsequent qRT-PCR analysis

showed that the BR negative-response genes *OsD2* and *OsD11* were down-regulated while *OsGATA6* was up-regulated (Supplementary Fig. S8A), suggesting that BR could induce *OsGATA6* expression. In panicle primordia at the In2–In3 stage, *OsD11* was up-regulated in the *OsGATA6*-AM line (Supplementary Fig. S8B), indicating a reduced BR signal as a result of *OsGATA6* knockdown. These data suggested that *OsGATA6* had the same regulatory orientation as the BR signal; however, the *OsGATA6* overexpression lines and genome-edited lines did not show different responses to BR treatment (Supplementary Fig. S8C).

We then transformed the *OsGATA6* overexpression vector into the Arabidopsis BR-insensitive mutant *bri1-5*. Overexpression of *OsGATA6* could partially rescue the *bri1-5* phenotype, and led to larger and flatter rosette leaves and a longer inflorescence stem (Supplementary Fig. S8D). However, across three independent transgenic lines of Arabidopsis, the BR negative-response genes *AtCPD* and *AtDWF4* were mostly up-regulated (Supplementary Fig. S8E). This indicated that the overexpression of *OsGATA6* did not induce the BR signal directly, and the rescue of plant growth and development probably occurred in a BR-independent or indirect manner, and very possibly acted downstream of the BR signal.

Discussion

In rice, *OsGATA6* is constitutively and strongly expressed in young panicles. Our GUS staining analyses indicated that *OsGATA6* showed a gradient of expression levels in developing young panicles (Supplementary Fig. S2C), which was slightly different from the expression pattern predicted from the Rice eFP Browser. This might be because the standard length of the panicle and the panicle developmental period vary among different rice cultivars. The dynamic expression of *OsGATA6* during panicle development is indicative of its function in regulating grain number per panicle. *In situ* hybridization analyses revealed that expression of *OsGATA6* was specifically localized in superficial cells of the panicle primordia (Supplementary Fig. S2D–G), suggesting that it might function in branch initiation. In the root tip, the transcripts of *OsGATA6* predominantly accumulate in the center of the root apical meristem (Zhang *et al*, 2021). Hence, *OsGATA6* is expressed in both shoot and root meristems; however, the specific locations result in different functions.

OsGATA6 encodes a putative transcription factor with multiple functions in regulating rice growth and grain yield. Its expression affected heading date, grain number per panicle, and grain size (Figs 1, 3, 4), and these three different traits appeared to be connected. We hypothesize that the primary function of OsGATA6 is the negative regulation of heading. Panicle development and architecture, the number of branches and spikelets, and the grain number per panicle are promoted by later heading, and a more extended period of vegetative growth results in greater accumulation of nutrients. There is a close relationship between grain number and grain size (Xue *et al.*, 2008; Wei *et al.*, 2010), and previous studies have reported that size is negatively affected by number because of overcrowding within the branches and spikelets. Our results showed that, compared with the wild-type ZH11, the *OsGATA6* overexpression (-OX) lines had more but smaller grains whilst the *OsGATA6* artificial microRNA interference (-AM) and *OsGATA6* CRISPR-Cas9 edited (-CRI) lines had fewer but larger grains.

Our results indicated that grain size was non-specifically or indirectly affected by *OsGATA6* and mainly determined by grain number because of limited space and nutrients. We also found *OsGATA6* affected grain size through influencing cell division since cell size was unaffected (Supplementary Fig. S7), which is worthy of further investigation. Too few seeds might result in wasted space within the panicle, whilst too many will increase the frequency of empty seeds because of insufficient nutrients, both of which will reduce yield. Enhancing grain yield by overexpression of *OsGATA6* would be theoretically possible because the decreased grain weight did not offset the increased grain number. On the other hand, OsGATA6 regulated grain shape and thus affected the visual quality, which potentially provides new options for rice breeders. Taken together, the increased grain number and altered grain shape resulting from overexpression of *OsGATA6* could be used in combination with other rice traits to breed new varieties with enhanced yield and different appearance.

OsGATA6 may affect heading in many ways. In the *OsGATA6*-OX and *OsGATA6*-AM transgenic lines there were changes in the transcript levels of several genes involved in the regulation of heading date, such as *RFT1*, *Hd3a*, and *OsMFT1*. Compared with the wild type, the transcript levels of *RFT1* and *Hd3a* were significantly reduced in the leaves of the *OsGATA6*-OX lines and increased in the *OsGATA6*-AM and *OsGATA6*-CRI lines (Fig. 1F). Increasing the transcript levels of *RFT1* in *OsGATA6*-OX led to the early heading of progeny plants (Supplementary Fig. S4B), and this complemented the late-heading phenotype of *OsGATA6*-OX lines; however, the excessive amounts of RFT1 caused the progeny plants to head too early. We also used dual-luciferase assays to detect the transcriptional regulation of *RFT1* and *Hd3a* by OsGATA6; however, there was no significant difference between OsGATA6 and the negative control (Supplementary Fig. S9), suggesting that OsGATA6 regulates *RFT1* and *Hd3a* via influencing their transcription indirectly.

Many candidate genes were identified downstream in the *OsGATA6*-AM transgenic lines, including *OsMFT1* (Fig. 5F), which encodes a protein with multiple functions in regulating rice heading date and panicle development (Song *et al.*, 2018). We found that OsGATA6 directly targeted the promoter region of *OsMFT1* (Fig. 5F) and induced its transcription, which provides a reasonable explanation for the phenotypes of the *OsGATA6* transgenic lines. OsGATA6 also delayed heading date by inhibiting the transcript levels of *RFT1* and *Hd3a*; however, it is also possible that it regulates heading date, grain number and size via other mechanisms as well (Fig. 7).

The function of OsGATA6 in regulating flowering time appeared to be similar between rice and Arabidopsis. In the rice *OsGATA6*-OX lines, the transcript levels of the florigens *RFT1* and *Hd3a* were significantly reduced, leading to late heading (Fig. 1F), whilst in Arabidopsis transcript levels of *AtFT*, the homolog of *RFT1*, were also reduced by the expression of *OsGATA6* (Fig. 2F), indicating that the two species shared similar regulatory mechanisms. Another gene related to flowering, *AtFLC*, was significantly up-regulated in the rosette leaves of the Arabidopsis *OsGATA6*-OX lines (Fig. 2E). The changes in the expression patterns of *AtFLC* and *AtFT* corresponded to a late-flowering phenotype, indicating that OsGATA6 regulated flowering time in Arabidopsis via the expression of these genes.

OsGATA6 is a close homolog of *OsGATA7* (Reyes *et al.*, 2004; Zhang *et al.*, 2018) and Arabidopsis *AtGATA2* (Reyes *et al.*, 2004; Luo *et al.*, 2010). The early-heading phenotype of the *OsGATA6*-AM and *OsGATA6*-CRI lines seemed to be weaker than late-heading phenotype of *OsGATA6*-OX (Fig. 1B), indicating the putative functional redundancy of homologous genes. Whether OsGATA7 or other homologs interact with OsGATA6 and synergistically affect heading date needs further study. *AtGATA2* and *OsGATA7* are involved in BR signaling, with *OsGATA7* being induced by BR, while *AtGATA2* is suppressed (Luo *et al.* 2010; Zhang *et al.* 2018). We checked the BR responses of *OsGATA6* expression together with BR signals in plants with modified *OsGATA6* expression. The expression of BR-related genes was affected in the *OsGATA6*-AM lines (Supplementary Fig. S8B). In addition, overexpression of *OsGATA6* partially rescued the phenotype of the Arabidopsis BR mutant *bri1-5* (Supplementary Fig. S8D). These results suggested that OsGATA6 and BR signals interacted in some processes; however, there was no difference in sensitivity to BR treatment between the rice *OsGATA6*-OX and *OsGATA6*-CRI lines (Supplementary Fig. S8C), and the transcript abundance of genes negatively regulated by BR did not show corresponding changes in the Arabidopsis *bri1-5* lines expressing *OsGATA6* (Supplementary Fig. S8E). These results suggested that *OsGATA6* functions in a BR-independent or indirect manner and possibly acts downstream of the BR signal.

Overall, our results show that OsGATA6 has multiple functions in regulating rice heading date and grain number per panicle. Consequently, it is a potential target to modify yield in future rice breeding programs.

Supplementary data

The following supplementary data are available at *JXB* online.

Fig. S1. Gene and protein structures of *OsGATA6*.

Fig. S2. Expression patterns and subcellular localization of *OsGATA6* transcripts.

Fig. S3. Genotyping of the *OsGATA6*-OX and *OsGATA6*-AM lines.

Fig. S4. Heading dates of the ZH11 wild-type and the *pOsGATA6::OsGATA6-GFP* and *OsGATA6*-OX/*RFT1*-OX lines.

Fig. S5. Relative transcript levels of key heading-date genes.

Fig. S6. Grain size in the ZH11 wild-type and the *OsGATA6*-OX, *OsGATA6*-AM, and *OsGATA6*-CRI lines.

Fig. S7. Cell length of lemmas in the ZH11 wild-type and the *OsGATA6*-OX, *OsGATA6*-AM, and *OsGATA6*-CRI lines.

Fig. S8. *OsGATA6* and brassinosteroid-mediated growth regulation in rice and Arabidopsis.

Fig. S9. Dual-luciferase assays of *RFT1* and *Hd3a* expression.

Table S1. List of the primers used in this study.

Table S2. List of the differentially expressed genes as determined by microarray analysis.

Acknowledgements

We thank Mr Hua Wang of Prof. Lin Xu's group (CEMPS) for help with the *in situ* experiment, and Ms Hong-Qin Gong of Prof. Hong-Wei Xue's group (CEMPS) for rice transformation.

Author contributions

WHL designed the project; YJZ, YZ, and LLZ performed the experiments; YJZ, WHL, and YZ analysed the data; WHL and YJZ wrote and edited the manuscript; JXH, HWX, and JWW provided useful discussions and helped editing the manuscript.

Conflict of interest

The authors declare that they have no conflicts of interest in relation to this work.

Funding

This work was supported by the National Natural Science Foundation of China (NSFC, Grant Nos 31761163003 and 90817009 to WHL, and 32000222 to YJZ), the Ministry of Agriculture of China (2009ZX08009-022B and 2008ZX08009-003 to WHL), the National Basic Research Program of China (2014CB943404 to WHL) and the Agri-X Interdisciplinary Fund of Shanghai Jiao Tong University (Agri-X20200204, to WHL), and by Project MDS-JF-2020-8 supported by the Shanghai Jiao Tong University JiRLMDS Joint Research Fund (to WHL) and the NSFC-Research Grants Council of Hong Kong (RGC) Joint Scheme (Ref.# N_CUHK452/17, to JXH).

Data availability

The data obtained from the microarray analysis are available in the NCBI database under accession number GSE199873. All other data supporting the findings of this study are available within the manuscript and its supplementary data published online.

References

Amasino R. 2010. Seasonal and developmental timing of flowering. The Plant Journal **61**, 1001–1013.

Brambilla V, Fornara F. 2013. Molecular control of flowering in response to day length in rice. Journal of Integrative Plant Biology **55**, 410–418.

Chardon F, Damerval C. 2005. Phylogenomic analysis of the PEBP gene family in cereals. Journal of Molecular Evolution **61**, 579–590.

Chen J, Gao H, Zheng XM, *et al*. 2015. An evolutionarily conserved gene, *FUWA*, plays a role in determining panicle architecture, grain shape and grain weight in rice. The Plant Journal **83**, 427–438.

Chu MX, Li JJ, Zhang JY, Shen SF, Li CN, Gao YJ, Zhang SQ. 2017. AtCaM4 interacts with a Sec14-like protein, PATL1, to regulate freezing tolerance in Arabidopsis in a CBF-independent manner. Journal of Experimental Botany **69**, 5241–5253.

Endo-Higashi N, Izawa T. 2011. Flowering time genes *Heading date 1* and *Early heading date 1* together control panicle development in rice. Plant & Cell Physiology **52**, 1083–1094.

Fornara F, Montaigu A, Coupland G. 2010. SnapShot: Control of flowering in Arabidopsis. Cell **141**, 550–550.e2.

Gu M, Zhang J, Li H, Meng D, Li R, Dai X, Wang S, Liu W, Qu H, Xu G. 2017. Maintenance of phosphate homeostasis and root development are coordinately regulated by MYB1, an R2R3-type MYB transcription factor in rice. Journal of Experimental Botany **68**, 3603–3615.

Hayama R, Izawa T, Shimamoto K. 2002. Isolation of rice genes possibly involved in the photoperiodic control of flowering by a fluorescent differential display method. Plant & Cell Physiology **43**, 494–504.

He P, Wang X, Zhang X, *et al*. 2018. Short and narrow flag leaf1, a GATA zinc finger domain-containing protein, regulates flag leaf size in rice *Oryza sativa*. BMC Plant Biology **18**, 273.

Huang R, Jiang L, Zheng J, Wang T, Wang H, Huang Y, Hong Z. 2013. Genetic bases of rice grain shape: so many genes, so little known. Trends in Plant Science **18**, 218–226.

Huang X, Qian Q, Liu Z, Sun H, He S, Luo D, Xia G, Chu C, Li J, Fu X. 2009. Natural variation at the *DEP1* locus enhances grain yield in rice. Nature Genetics **41**, 494–497.

Hudson D, Guevara DR, Hand AJ, Xu Z, Hao L, Chen X, Zhu T, Bi YM, Rothstein SJ. 2013. Rice cytokinin GATA Transcription Factor1 regulates chloroplast development and plant architecture. Plant Physiology **162**, 132–144.

Ikeda K, Nagasawa N, Nagato Y. 2005. ABERRANT PANICLE ORGANIZATION 1 temporally regulates meristem identity in rice. Developmental Biology **282**, 349–360.

Ikeda K, Sunohara H, Nagato Y. 2004. Developmental course of inflorescence and spikelet in rice. Breeding Science **54**, 147–156.

Jain M, Nijhawan A, Arora R, Agarwal P, Ray S, Sharma P, Kapoor S, Tyagi AK, Khurana JP. 2007. F-box proteins in rice: genome-wide analysis, classification and spatial and temporal gene expression during panicle and seed development and regulation by light and abiotic stress. Plant Physiology **143**, 1467–1483.

Jiang WB, Huang HY, Hu YW, Zhu SW, Wang ZY, Lin WH. 2013. Brassinosteroid regulates seed size and shape in Arabidopsis. Plant Physiology **162**, 1965–1977.

Komatsu M, Maekawa M, Shimamoto K, Kyozuka J. 2001. The *LAX1* and *FRIZZY PANICLE2* genes determine the inflorescence architecture of rice by controlling rachis-branch and spikelet development. Developmental Biology **231**, 364–373.

Komiya R, Yokoi S, Shimamoto K. 2009. A gene network for long-day flowering activates *RFT1* encoding a mobile flowering signal in rice. Development **136**, 3443–3450.

Li D, Wang L, Wang M, Xu YY, Luo W, Liu YJ, Xu ZH, Li J, Chong K. 2009. Engineering *OsBAK1* gene as a molecular tool to improve rice architecture for high yield. Plant Biotechnology Journal **7**, 791–806.

Li F, Liu W, Tan J, Chen J, Tong H, Hu B, Li C, Fang J, Chen M, Chu C. 2010. Rice DENSE AND ERECT PANICLE2 is essential for determining panicle outgrowth and elongation. Cell Research **20**, 838–849.

Li N, Li Y. 2016. Signaling pathways of seed size control in plants. Current Opinion in Plant Biology **33**, 23–32.

Li N, Zhang DS, Liu HS, *et al*. 2006. The rice *Tapetum Degeneration Retardation* gene is required for tapetum degradation and anther development. The Plant Cell **18**, 2999–3014.

Li QQ, Zhang Z, Wang YL, Zhong LY, Chao ZF, Gao YQ, Han ML, Xu L, Chao DY. 2021. Phytochrome B inhibits darkness-induced hypocotyl adventitious root formation by stabilizing IAA14 and suppressing ARF7 and ARF19. The Plant Journal **105**, 1689–1702.

Liu W, Xu ZH, Luo D, Xue HW. 2003. Roles of OsCKI1, a rice casein kinase I, in root development and plant hormone sensitivity. The Plant Journal **36**, 189–202.

Lowry JA, Atchley WR. 2000. Molecular evolution of the GATA family of transcription factors: conservation within the DNA-binding domain. Journal of Molecular Evolution **50**, 103–115.

Lu G, Casaretto JA, Ying S, Mahmood K, Liu F, Bi YM, Rothstein SJ. 2017. Overexpression of OsGATA12 regulates chlorophyll content, delays plant senescence and improves rice yield under high density planting. Plant Molecular Biology **94**, 215–227.

Luo XM, Lin WH, Zhu S, *et al*. 2010. Integration of light- and brassinosteroid-signaling pathways by a GATA transcription factor in Arabidopsis. Developmental Cell **19**, 872–883.

Miao J, Guo D, Zhang J, Huang Q, Qin G, Zhang X, Wan J, Gu H, Qu LJ. 2013. Targeted mutagenesis in rice using CRISPR-Cas system. Cell Research **23**, 1233–1236.

Nemoto Y, Nonoue Y, Yano M, Izawa T. 2016. *Hd1*, a *CONSTANS* ortholog in rice, functions as an *Ehd1* repressor through interaction with monocot-specific CCT-domain protein Ghd7. The Plant Journal **86**, 221–233.

Reyes JC, Muro-Pastor MI, Florencio FJ. 2004. The GATA family of transcription factors in Arabidopsis and rice. Plant Physiology **134**, 1718–1732.

Sakamoto T, Matsuoka M. 2008. Identifying and exploiting grain yield genes in rice. Current Opinion in Plant Biology **11**, 209–214.

Song Q, Huang TY, Yu HH, Ando A, Mas P, Ha M, Chen ZJ. 2019. Diurnal regulation of *SDG2* and *JMJ14* by circadian clock oscillators orchestrates histone modification rhythms in Arabidopsis. Genome Biology **20**, 170.

Song S, Wang G, Hu Y, Liu H, Bai X, Qin R, Xing Y. 2018. *OsMFT1* increases spikelets per panicle and delays heading date in rice by suppressing *Ehd1*, *FZP* and *SEPALLATA*-like genes. Journal of Experimental Botany **69**, 4283–4293.

Subaran S, Anupriya S, Ashis KN. 2016. The rice *OsSAG12-2* gene codes for a functional protease that negatively regulates stress-induced cell death. Journal of Biosciences **41**, 445–453.

Takashi A, Yoshibumi K. 1993. Analysis of the role of the late-flowering locus, *GI*, in the flowering of *Arabidopsis thaliana*. The Plant Journal **3**, 231–239.

Tamaki S, Matsuo S, Wong HL, Yokoi S, Shimamoto K. 2007. Hd3a protein is a mobile flowering signal in rice. Science **316**, 1033–1036.

Wang LP, Yin HF, Qian Q, Yang J, Huang CF, Hu XH, Luo D. 2009. NECK LEAF 1, a GATA type transcription factor, modulates organogenesis by regulating the expression of multiple regulatory genes during reproductive development in rice. Cell Research **19**, 598–611.

Warthmann N, Chen H, Ossowski S, Weigel D, Hervé P. 2008. Highly specific gene silencing by artificial miRNAs in rice. PLoS ONE **3**, e1829.

Wei X, Xu J, Guo H, Jiang L, Chen S, Yu C, Zhou Z, Hu P, Zhai H, Wan J. 2010. *DTH8* suppresses flowering in rice, influencing plant height and yield potential simultaneously. Plant Physiology **153**, 1747–1758.

Xing MQ, Wang W, Fang X, Xue HW. 2022. Rice OsIAA6 interacts with OsARF1 and regulates leaf inclination. The Crop Journal. In Press, doi:10.1016/j.cj.2022.02.010.

Xing Y, Zhang Q. 2010. Genetic and molecular bases of rice yield. Annual Review of Plant Biology **61**, 421–442.

Xue W, Xing Y, Weng X, *et al*. 2008. Natural variation in *Ghd7* is an important regulator of heading date and yield potential in rice. Nature Genetics **40**, 761–767.

Zeevaart JAD. 2006. Florigen coming of age after 70 years. The Plant Cell **18**, 1783–1789.

Zhang S, Hu W, Wang L, Lin C, Cong B, Sun C. 2005. *TFL1/CEN*-like genes control intercalary meristem activity and phase transition in rice. Plant Science **168**, 1393–1408.

Zhang TQ, Chen Y, Liu Y, Lin WH, Wang JW. 2021. Single-cell transcriptome atlas and chromatin accessibility landscape reveal differentiation trajectories in the rice root. Nature Communications **12**, 2053.

Zhang YJ, Zhang Y, Zhang LL, Huang HY, Yang BJ, Luan S, Xue HW, Lin WH. 2018. *OsGATA7* modulates brassinosteroids-mediated growth regulation and influences architecture and grain shape. Plant Biotechnology Journal **16**, 1261–1264.

Zheng T, Sun J, Zhou S, *et al*. 2019. Post-transcriptional regulation of Ghd7 protein stability by phytochrome and OsGI in photoperiodic control of flowering in rice. New Phytologist **224**, 306–320.

Zhou SR, Xue HW. 2020. The rice PLATZ protein SHORT GRAIN6 determines grain size by regulating spikelet hull cell division. Journal of Integrative Plant Biology **62**, 847–864.

Zhou S, Zhu S, Cui S, *et al*. 2021. Transcriptional and post-transcriptional regulation of heading date in rice. New Phytologist **230**, 943–956.

Zuo J, Li J. 2014. Molecular genetic dissection of quantitative trait loci regulating rice grain size. Annual Review of Genetics **48**, 99–118.